ISSN 1070-3632, Russian Journal of General Chemistry, 2013, Vol. 83, No. 11, pp. 2203–2211. © Pleiades Publishing, Ltd., 2013.
Original Russian Text © M.Yu. Tsvetkov, B.N. Khlebtsov, E.V. Panfilova, V.N. Bagratashvili, N.G. Khlebtsov, 2012, published in Rossiiskii Khimicheskii Zhurnal, 2012, Vol. 56, Nos. 1–2, pp. 83–90.

Gold Nanorods as a Perspective Technology Platform for SERS Analytics

M. Yu. Tsvetkov[a], B. N. Khlebtsov[b], E. V. Panfilova[b], V. N. Bagratashvili[a], and N. G. Khlebtsov[b,c]

[a] *Department of Perspective Laser Technologies, Institute for Laser and Information Technologies, Russian Academy of Sciences, Pionerskaya str. 2, Troitsk, Moscow, 142190 Russia*
e-mail: mtsvet52@mail.ru

[b] *Institute of Biochemistry and Physiology of Plants and Microorganisms, Russian Academy of Sciences (IBPPM RAS), Saratov, Russia*
e-mail: khlebtsov@ibppm.sgu.ru

[c] *Chernyshevskii Saratov State University, Saratov, Russia*
Received June 1, 2012

Abstract—We discuss the application of gold nanorods for forming SERS substrates for chemical and biological sensing. Two approaches are considered: (1) formation of planar arrays on silicon wafers by using suspensions of gold nanorods; and (2) a new approach based on gold nanorod powders that can be easily dissolved in aqueous media. Both SERS platforms are characterized and their SERS enhancement factors are compared.

DOI: 10.1134/S1070363213110406

INTRODUCTION

Raman spectroscopy has found wide application in chemistry, biology, and medicine [1–3]. This technique has long been used largely in basic research but presently, due to the progress in the instrumental base and data processing, it is becoming a commonly accepted method of molecular analysis [4]. Further progress of Raman spectroscopy is associated with the development of resonance Raman spectroscopy and, in particular, surface-enhanced Raman scattering (SERS) [2, 3, 5, 6]. The SERS spectroscopy is used in ultratrace analysis (up to detection of single molecules [7, 8]), surface research on "ordinary" materials and nanomaterials [9], structural research on macromolecules [10], as well as in biomedical diagnostics and other fields.

The principal mechanisms of SERS scattering are electromagnetic and chemical signal enhancement [5, 6], the first mechanism prevailing. Chemical enhancement is associated with the direct interaction of adsorbate molecules with metal (wafer) surface [2]. Electromagnetic enhancement is associated with the interaction of incident and scattered light either with a rough metal surface or with metal nanoparticles or their clusters. The electric field of electromagnetic waves excites in the metal collective electron oscillations called surface plasmons [11]. At certain optical frequencies, such oscillations are excited in the resonance, which entails substantial charge shifts and local electromagnetic field enhancements. This phenolmenon arises in metal nanoparticles and is referred to as localized surface plasmon resonance (LSPR) [11]. The intensity and frequency of LSPR are dependent on the shape and structure of the particle and its local environment [12]. In the case of clusters, the electromagnetic enhancement of SERS is due to the efficient electromagnetic interaction of nanoparticles, which takes place when they approach each other by a distance shorter than 10% of their diameter [13, 14]. As a result, the local field amplitude in the so-called hot spots can be enhanced by two orders of magnitude [6, 15], and the SERS signal, by eight orders of magnitude, since it is roughly proportional to the fourth degree of the incident light amplitude.

When doing SERS analysis, researchers commonly deal with an integral signal from a micron area of wafer surface. In this case, engineering and methodical

aspects, in particular, the technology of fabrication of SERS substrates, choice of metal for the substrate (usually silver or gold), parameters of substrate particles and structure, and methodology of SERS measurements and their reproducibility and standardization become of primary importance.

The progress of nanotechnologies open up new possibilities for the fabrication of metal nanoparticles with different shapes, sizes, and optical properties [12], as well as of different 1D, 2D, and 3D nanostructures [16] and composites [17], which can be used as a SERS platform. In the simplest case, Raman signal enhancement can be reached in a colloid solution of plasmon resonance nanoparticles [18]. Successful use of gold and silver nanospheres, nanocubes, nanoshells, nanocages, particles microaggregates, and other nanomaterials as substrate materials has been reported [16]. The most widespread are particle monolayers or planar nanostructures formed by self-assembly, nanolithography, or ion etching [19]. It should be noted that the search for optimal SERS platforms is far from being completed [20], and the research is in progress [17].

Nanostructures from anisotropic metal nanoparticles (gold and silver nanorods and nanowires) seem to be a promising platform for SERS spectroscopy by the following reasons. First, the plasmon resonance of such nanoparticles can be adjusted to a desired spectral range by varying the aspect ratio of nanorods [21]. Second, there is substantial field enhancement around nanoparticle ends in cases when the incident light polarization coincides with the particle axis [22]. Finally, reliable evidence of the synthesis of nonspherical particles with preset geometric and optical parameters is available [23–25]. Gold nanorods layers fabricated by polyionic assembly, ordered planar monolayers and fractal nanorod aggregates, and colloid quasicrystals packed orthogonally with respect to wafer surface was used as SERS platforms (see also references in [26]).

In the present work, we consider two engineering approaches to SERS platforms on the basis of gold nanorods. The first involves the deposition of monolayers of gold nanorods on single-crystalline silicon followed by the deposition of an analyte and registration and interpretation of the SERS spectrum [26]. We discuss here data obtained for three types of gold nanorod arrays: a rare monolayer, a densely packed monolayer, and a fractal film.

The second approach makes use of a new type of nanomaterials, viz. gold nanorod powders, for forming SERS platforms [27, 28]. Plasmonic nanopowders are perspective materials for SERS substrates as applied to chemical and biological sensing [27]. The principal advantages of this approach include the possibility of long-term storage of the powder and its quality control, reproducible preparation of highly concentrated nanoparticle suspensions (about 100 mg/mL for the gold nanoparticles), as well as joint deposition of the coating and analyte during substrate fabrication.

Gold Nanorod Monolayers as Substrates in the SERS Analysis

Two types of nanorods exhibiting plasmon resonances at 670 and 810 nm (further denoted as GNR-670 and GNR-810, respectively) were used to fabricate substrates of different structures. These nanorods were fabricated by the procedures described in [29, 30], modified to control the shape and aspect ratio of particles. The procedures for the fabrication of SERS substrates (gold nanorod layers) of different structures were described in detail in [26], and the procedures for the fabrication of powders of gold nanorods and particles of other shapes were reported in [27, 28].

Gold Nanorod Particle Parameters and Layer Structures

The geometry of particles and the structure of monolayers were determined from the images obtained by transmission electron microscopy (TEM) with a Libra-120 instrument (Carl Zeiss, Germany). The optical properties of nanoparticles and their suspensions were controlled by the absorption spectra obtained with a Specord 250 UV-vis spectrophotometer (Analytik Jena, 190–1100 nm).

Figure 1 shows the TEM images of rare monolayers of gold nanoparticles from the GNR-670 (a) and GNR-810 samples (b). As seen from the figure, the particles shape corresponds, on average, to hemisphere-ended cylinder, and the shape variations related to flattened ends and decreased central diameter of the particles (end-cap and dog-bone morphology [29]) are negligible.

For an ensemble of about 500 particles we determined the length L_i, diameter d_i, and aspect ratio $r_i = L_i/d_i$ of each particle. The average rod lengths and diameters in the GNR-670 sample (Fig. 1a) are as follows: L = 64.5±6 nm and d = 23±2.6 nm. The respective values for the GNR-810 sample (Fig. 1b)

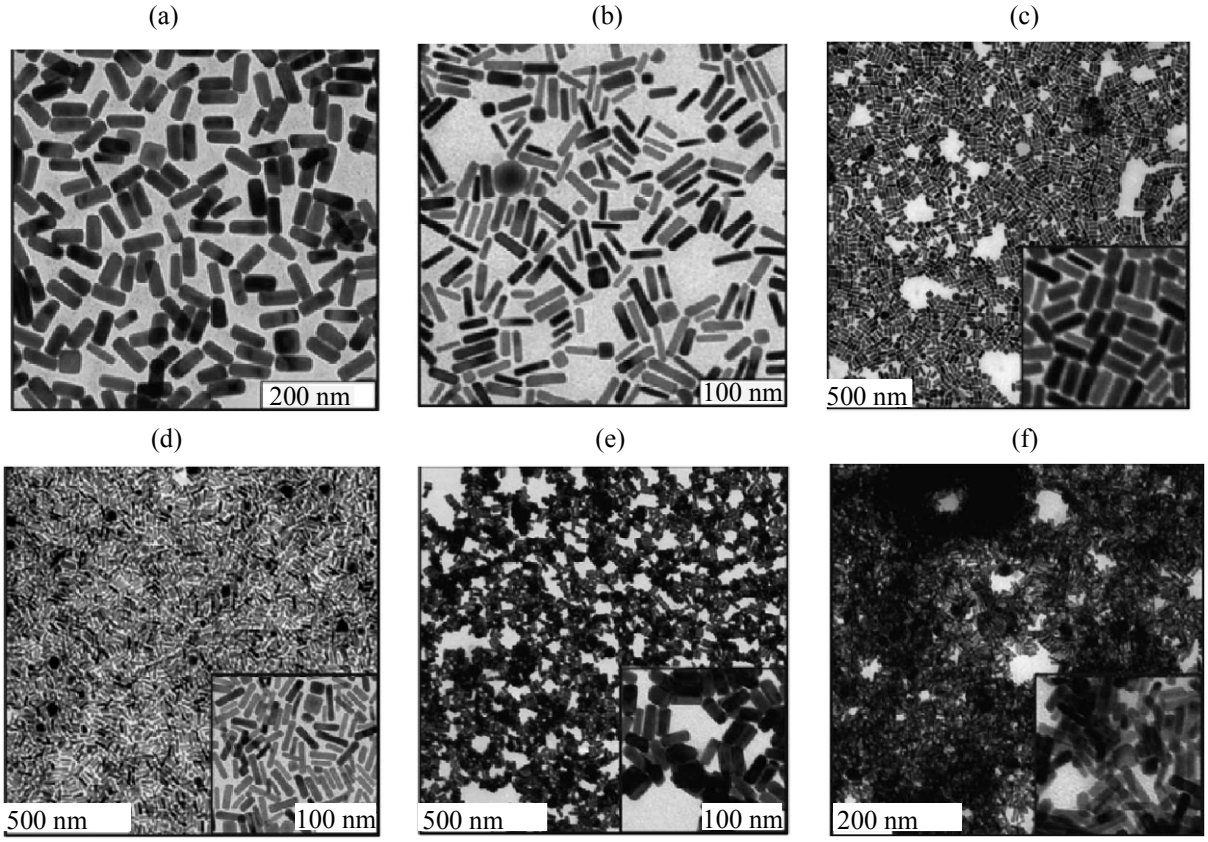

Fig. 1. Electron microscopic images of (a, b) rare particle monolyers, (c, d) densely packed nanoparticle monolayers, and (e, f) fractal films obtained from the samples (a, c, e) GNR-670 and (b, d, f) GNR-810.

are as follows: L = 45±8.5 nm and d = 11±1.8 nm. In view of the nanoparticle morphology and previous theoretical simulation data [29], we suggested that the nanoparticles with the above geometric parameters would have longitudinal plasmon resonances in the ranges 650–680 nm for GNR-670 and 800–830 nm for GNR-810; excellent agreement with the experiment was found.

As to the structure of the resulting nanoparticle layers, the packing density of the rare monolayer (estimated as the ratio of the surface area, occupied by nanoparticles, to the total wafer surface area) was 32 and 24% for the GNR-670 and GNR-810 samples, respectively, and the location and mutual arrangement of nanoparticles were random in nature.

Figure 1 also shows the overview and enlarged TEM images of densely packed nanoparticle monolayers and fractal films obtained from the GNR-670 and GNR-810 samples. The self-assembly of particles forms densely packed structures in which the distances between particles are much smaller than the geometric dimensions. In the case of self-assembly (Figs. 1c and 1d), a tendency for parallel side-by-side aggregation of nanoparticles and 2D film formation is observed. The number of particles in a unit chain with a parallel side-by-side packing varies from 2–3 to 5–6, and these chains are randomly oriented in the plane.

When a fractal film (Figs. 1e and 1f) is formed at the phase interface, the corresponding wafers do not have a monolyer packing and can be characterized as structures with a random 3D particle arrangement. Therewith, it is clear that the longitudinal extent of the film is much larger than its thickness. The TEM images of such films look like colloid fractal aggregate structures, which explains the fact that in the literature and our present work they are referred to as fractal films.

SERS Measurements Using Substrates with Gold Nanorod Monolayers

To test the efficiency of fabricated SERS substrates, we used Rhodamine 6G dye. A solution of this

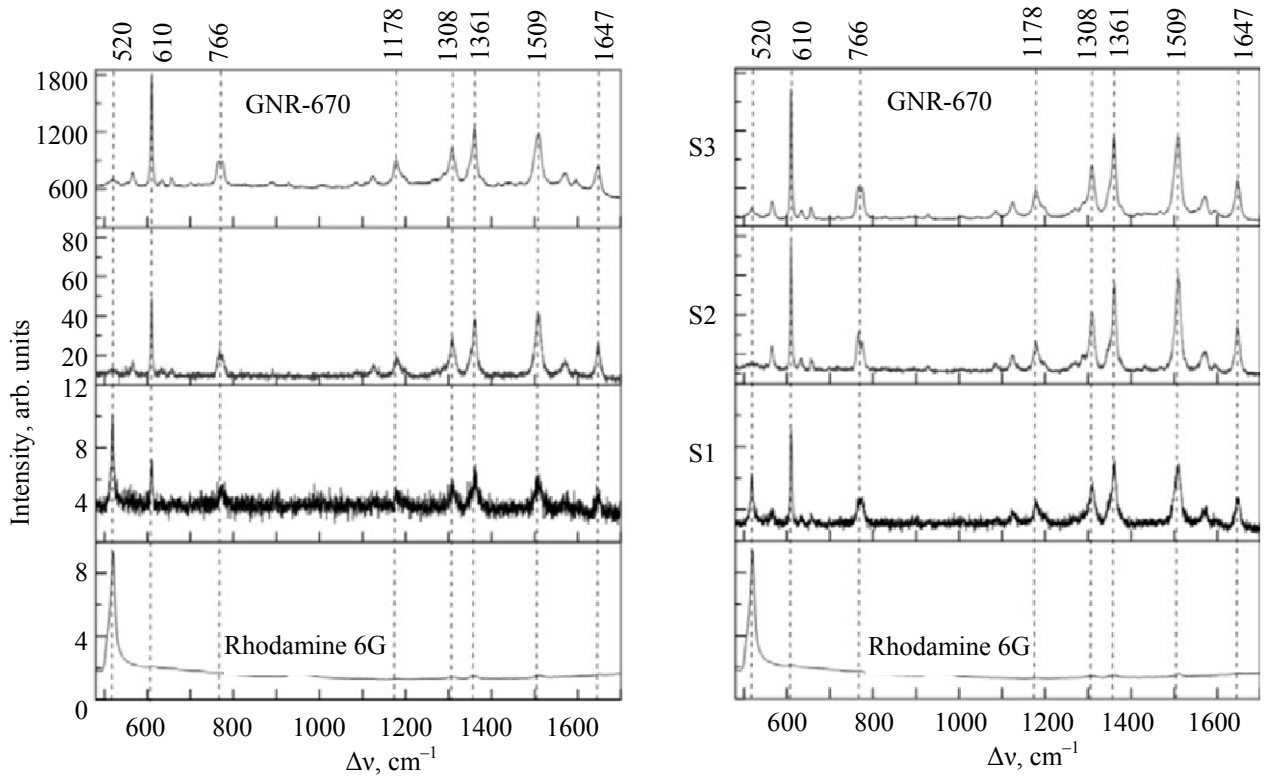

Fig. 2. SERS spectra of Rhodamine 6G, obtained at the wavelength 633 nm using (S1) rare and (S2) densely packed nanorod layers, and (S3) fractal film. Data for the GNR-670 and GNR-810 samples are presented; at the bottom, the spectra of Rhodamine 6G on a silicon wafer are shown for comparison.

dye in ethanol (concentration 80×10^{-6} M, 1 μL) was applied on the substrate surface. The average surface area occupied by the sample after its spreading was ~0.5 cm^2. The SERS signal was measured with a Horiba Jobin Yvon HR 800 instrument which combines a Raman spectrometer and a confocal microscope. The light source was a He–Ne laser (wavelength 632.8 nm, power 17 mW). The SERS enhancement of gold nanorods was studied at the incident light power of 80 μW, and to measure the Raman spectra of uncoated silicon wafers, the power was increased by two orders of magnitude (to 8 mW). The focus spot diameter was ~20 μm, and the signal acquisition time was 10 s (the signal was averaged over 10 measurements).

The efficiency of the synthesized substrates as a SERS platform was assessed from a comparison of the SERS spectra of Rhodamine 6G with the Raman spectrum of this dye on a silicon wafer. In agreement with published data on the Raman [31] and SERS spectra [32] of Rhodamine 6G, our measured spectra (Fig. 2) show well-defined maxima at 610, 766, 1178, 1306, 1361, 1509, and 1647 cm^{-1}, corresponding to C–H, C–O–C, and C–C vibrations. The spectra of the dye on a rare monolayer (S1 on Fig. 2) also contain a strong silicon band at 520 cm^{-1}. The corresponding band in the spectra measured from densely packed arrays (S2 and S3 in Fig. 2) is very weak. We suppose that the weakening of this band is associated with shielding of the wafer with a layer of particles with high absorption and scattering at the probe radiation wavelength. Note that the laser radiation power for measuring conventional Raman spectra (Fig. 2, bottom spectra) was increased 100 times, compared to that used for measuring SERS spectra. However, the signal intensity was found to be quite low, while the lines at 766 and 1647 cm^{-1} were absent at all.

Comparing the spectra in Fig. 2 we can draw a number of important conclusions. The fabricated SERS substrates efficiently enhance the Rhodamine 6G signal. The SERS signal enhancement increases by orders of magnitude as nanorods get closer to each other and more densely packed. For example, the intensity of the signal at 610 cm^{-1} in the spectrum of

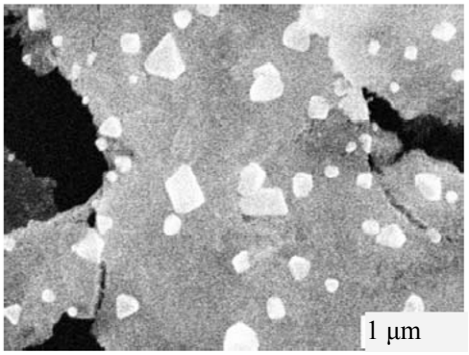

Fig. 3. Electron microscopic image of a fractal film, illustrating nanoparticle aggregation.

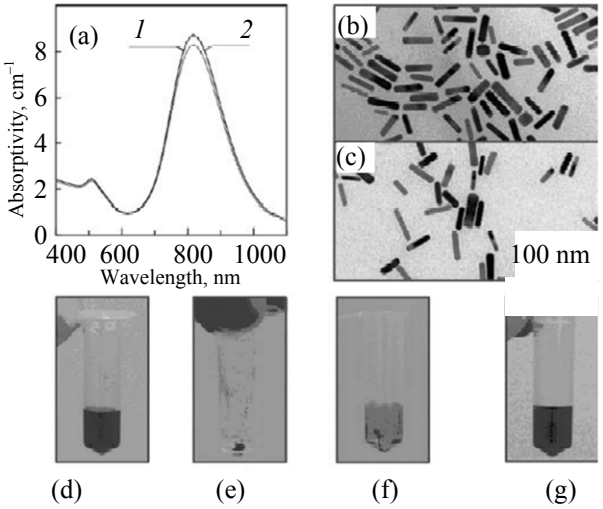

Fig. 4. (a) Absorption spectra of the (*1*) starting gold nanorods and (*2*) resuspended powder and electron microscopic images of gold nanorods (b) before freeze-drying and (c) after dissolution in water. The images at the bottom show (d) suspension of freshly prepared gold nanorods, (e) freeze-dried powder, (f) solution immediately after adding water, and (g) suspension of gold nanorods after slight shaking for a few seconds.

the dye on an unpacked GNR-670 Array is 7 arb. units; the respective values for the dye on a monolayer with the particle-to-particle distance of 1–3 nm and a fractal film are 80 and 1800 rel. units. The average SERS signal enhancement at on 400-μm^2 portions of the fractal film was estimated at 10^5–10^6; the line intensity reproducibility was ~10% over different portions of the substrate. The strong enhancement in fractal films of nanorods agrees with the previous observation of field hot spots in such structures [15]. However, it should be borne in mind that our estimates are semiquantitative, since different 20×20 μm^2 portions contained different numbers of particles and, possibly, different numbers of molecules. No essential difference in the intensity of the SERS spectra measured with arrays of nanorods of different aspect ratios was observed (in any case, the differences were not systematic). The SERS signal was higher in the case of the monolayer of GNR-810 nanorods with a large aspect ratio, and GNR-670 fractal films showed a slightly stronger enhancement.

Problem of Substrate Aging

The key problems associated with the analytical application of SERS spectroscopy are stability of SERS substrates and reproducibility of measurements under different conditions. Our research showed that SERS substrates are subject to aging (Natan [20] has recently called attention to this problem). The aging effect is due, in particular, to gold or silver nanoparticle aggregation processes (Fig. 3) which entail gradual reduction of the SERS enhancement factor. Fractal films are the most susceptible to aging: The SERS intensity from fractal films decreases within 1–2 months to reach the intensity level of signals from densely packed films (this finding implies that only freshly prepared fractal films are suitable for operation). The SERS intensity from densely packed films remains at an acceptable level for a few months. Substrate aging restricts extensive use of the SERS technique.

Gold Nanorod Powders as a Platform for SERS Spectroscopy

The problem of substrate aging can be avoided if SERS substrates from plasmonic gold nanoparticle powders are fabricated directly during experiment [27]. Such nanomaterials can be stored for a long time under general conditions. Absorption spectroscopy and electron microscopy of diluted and initial colloid solutions of gold nanorods revealed no essential difference (Figs. 4a and 4b). Preliminary observations [27] showed that the plasmonic properties of the powder had not changed during its storage for 9 months at room temperature.

The procedure of the SERS experiment with nanopowders consists in directly suspending a portion of nanopowder in an analyte solution, drying the resulting suspension on a silicon wafer, and SERS measurements. This procedure allows the two steps of key importance for SERS, specifically, fabrication of the substrate and uniform deposition of the analyte, to be combined in one step. A modification of the

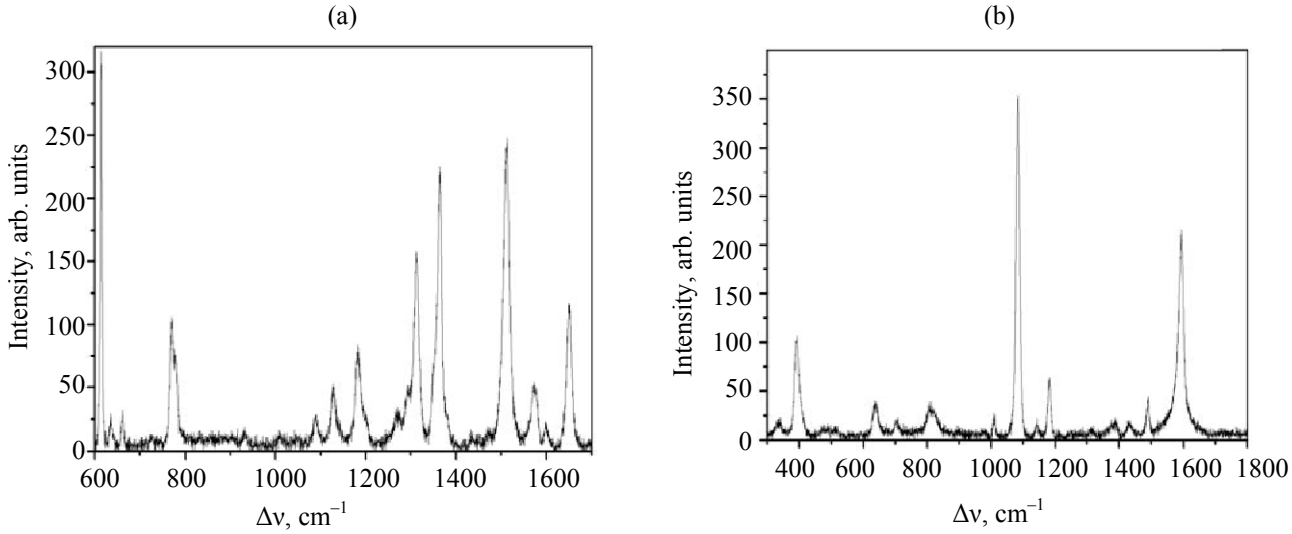

Fig. 5. SERS spectra of (a) Rhodamine 6G and (b) 4-aminothiophenol, obtained using gold nanopowders.

procedure is possible: The powder is suspended in a small volume of a solvent to a desired concentration, after which an aliquot of an analyte solution is mixed with an aliquot of a dissolved powder suspension ("drop+drop"), and the mixture is deposited on a silicon wafer. In the latter version, one portion of the powder (in our case, 0.3–0.5 mg) is used to prepare several samples.

SERS Measurements with Gold Nanorod Powders

4-Aminothiophenol (Fig. 5b) was used as one more test analyte, along with Rhodamine 6G (Fig. 5a), in SERS measurements on gold nanorod substrates. This compound readily binds to gold nanoparticles by Au–S bonds and is therefore widely used in spectral studies [33].

The Raman spectrum of 4-aminothiophenol contains well-defined characteristic bands, the most characteristic of which are C–S (1077 cm^{-1}) and C–C (1576 cm^{-1}) vibration bands. Moreover, both electromagnetic and chemical SERS enhancement is observed.

4-Aminothiophenol was used to optimize the concentration of aqueous suspensions of SERS powders. Figure 6a shows the relative intensities of the SERS signal of this test analyte in the aqueous suspensions. Because of the lack of thorough control of the thickness of SERS coating in the present work, we can draw now only preliminary conclusions. There is an optimal concentration range of gold nanorods (10–20 mg/mL), which allows a maximum SERS enhancement with a small variation within the range. At such concentrations, the spots of a dried suspension have a characteristic golden color. At higher concentrations SERS enhancements decreases, which appears to be associated with shielding effects arising from the multilayer packing of gold nanorods. When the concentration of 4-aminothiophenol is lower than optimal, the SERS signal decreases essentially due to the decrease of plasmon enhancement of local fields with increasing the average interparticle distances. Consequently, the signal from diluted systems is formed by individual gold nanorods, and the electromagnetic enhancement is single-particle in nature.

SERS Enhancement Factor

The key parameter of SERS spectroscopy is the enhancement factor [34]. This parameter is quite difficult to measure, because, on the one hand, the intensities of Raman and SERS signals differ from each other by several orders of magnitude, and, on the other, the SERS process depends of a great number of factors which are hardly accountable experimentally. Therefore, this problem still has to be solved and is actively discussed in special literature. Different experimental approaches to measuring the SERS enhancement factor have been proposed. Their most comprehensive analysis can be found in [34] (see also the monograph [6]).

From the practical viewpoint, correct integral values of the SERS enhancement factor can only be obtained if the number of variables is as small as possible. In particular, this can be reached by varying the concentration of the test analyte only, whereas all geometric parameters of the measurement system and

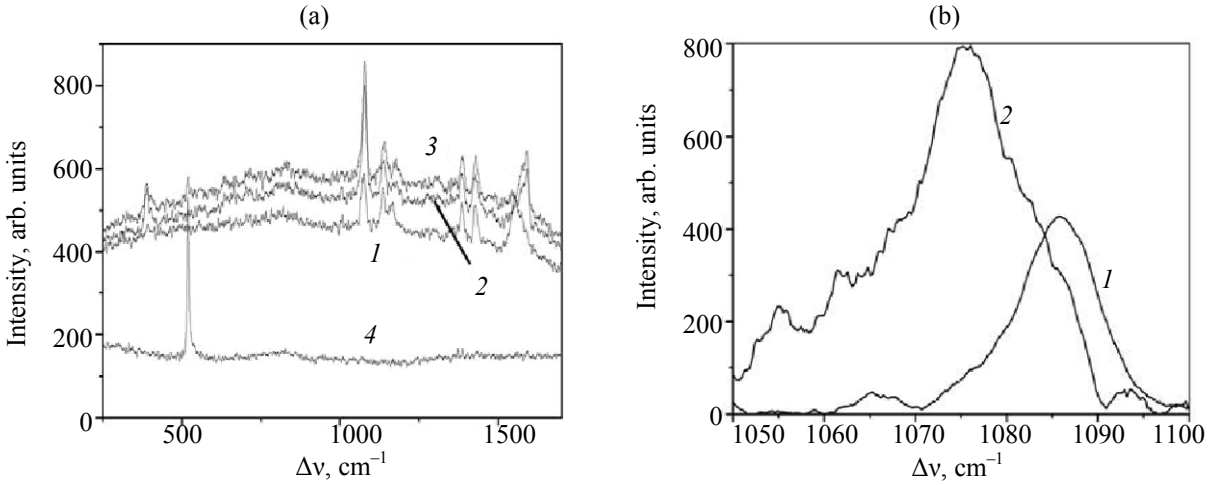

Fig. 6. (a) Relative intensities of SERS signals at varied concentrations of a 4-aminothiophenol test analyte in aqueous solutions and results of measurement of the SERS enhancement factor with the same test analyte. (a) Solution concentration, mg/mL: (*1*) 48, (*2*) 24, (*3*) 12, and (*4*) 6. (b): Signal: (*1*) Raman and (*2*) SERS.

conditions of spectrum excitation remain unchanged. Then for the "practical" enhancement factor we can accept the ratio of the SERS and Raman signals, multiplied by the ratio of the corresponding concentration. In our case the analyte concentrations were 100 mM for Raman measurements and 80 μM for SERS measurement, and the ratio of the measured signals was 2 (Fig. 6b). Under these conditions, the practical enhancement factor is

$$K = (100\ \text{mM}/80\ \mu\text{M})\cdot 2 = 2500.$$

It should be emphasized again that the enhancement factor we discuss here is purely practical in meaning: It tells us how many times one can dilute an analyte for its SERS signal to compare in intensity with the Raman signal for the undiluted analyte. This approach ignores the question of the real number of molecules contributing into the measured spectral signal, but is commonly accepted in determining the SERS enhancement factor with account for molecular orientation and other factors [34]. However, detailed analysis shows [34] that in practice the SERS enhancement factor for self-assembled wafers of nanoparticles is quite difficult to determine correctly. Possibly, this fact explains a considerable scatter (several orders of magnitude) in the reported estimates for the electromagnetic and chemical contributions into the total SERS enhancement [20, 34].

The key problem in SERS measurements is to obtain a reliably registered signal. This is only possible at sufficiently high analyte concentrations. Therewith, one has to provide a sufficiently uniform surface of the spot of a dry analyte suspension. At the same time, the above conditions should be so that to prevent photodegradation of the analyte during SERS measurements. In our experiment (Fig. 6b), measurements were performed within "one spectral scan" (1024 cells of the CCD matrix) to ensure a minimum heating of the sample. Comparison was performed by the signals at 1087 (1077) cm^{-1}. In particular, this fact shows that SERS spectra differ from Raman spectra both by the intensity of spectral lines and by certain spectral shifts.

The resulting integral SERS enhancement factor (~2500) is close to values reported for commercial SERS wafers (still few in number; see, for example, [35], where the electromagnetic SERS enhancement factor of 10^4 is reported). At the same time, the use of nanopowders solves the problem of temporary stability and availability of plasmonic media.

CONCLUSIONS

Further progress in the field of SERS platforms is associated with the diversity of applications of SERS substrates and no universal solution is expected. The development of quantitative SERS calls for substrates with a uniform surface and stable and reproducible parameters. Such substrates are fabricated by electrochemical, vacuum, and other methods. Over the past years the most progress has been made in nanolithography which provides an efficient technology for fabricating substrates with an exactly reproducible structure.

Highly demanded are analytical applications of SERS spectroscopy, when express measurements should be carried out of a dedicated laboratory and for low cost. In view of the recent advent of portable Raman spectrometers to the instrumental market, we can expect that gold nanorod powders will occupy their niche as a low-cost and convenient SERS platform for analytical purposes.

ACKNOWLEDGMENTS

The work was financially supported in part by the Russian Foundation for Basic Research (project nos. 11-02-12087, 11-02-00128a, and 12-02-00379a), Research and Pedagogical Personnel of Innovative Russia Federal Targeted Program (State Contract 14.740.11.0260), Grant of the President of the Russian Federation to support young candidates of sciences (grant no. MK-1057.2011.2), as well as Grant of the Government of the Russian Federation to support scientific research projects implemented under the supervision of leading researchers at the Russian institutions of higher education.

The authors are grateful to A.M. Burov (IBPPM RAS) and M.A. Timofeev (Research Institute of Nuclear Physics, Moscow State University) for help in electron microscopic measurements.

REFERENCES

1. Fabelinskii, I.L., *Soviet Physics-Uspekhi*, 1978, vol. 126, p. 780.
2. Kosuda, K.M., Bingham, J.M., Wustholz, K.L., and Van Duyne, R.P., *Comprehensive Nanoscience and Technology,* 2011, vol. 3, pp. 263–301.
3. Cialla, D., März, A., Böhme, R., Theil, F., Weber, K., Schmitt, M., and Popp, J., *Anal. Bioanal. Chem*., 2012, vol. 403, pp. 27–54.
4. Pentin, Yu.A. and Vilkov, L.V., *Fizicheskie metody issledovaniya v khimii* (Physical Methods in Chemistry), Moscow: Mir, 2009.
5. Moskovits, M., *Rev. Mod. Phys*., 1985, vol. 57, pp. 783–826.
6. Le Ru, E.C. and Etchegoin, P.G., *Principles of Surface Enhanced Raman Spectroscopy*, Amsterdam: Elsevier, 2009.
7. Kneipp, K., Wang, Y., Kneipp, H., Perelman L.T., Itzkan, I., Dasari, R.R., and Feld, M.S., *Phys. Rev. Lett*., 1997, vol. 78, pp. 1667–1670.
8. Nie, S. and Emory, S.R., *Science*, 1997, vol. 275, pp. 1102–1106.
9. Gouadec, G. and Colomban, P., *Prog. Cryst. Growth Charact. Mater*., 2007, vol. 53, pp. 1–56.
10. Qian, X.-M. and Nie, S.M., *Chem. Soc. Rev*., 2008, vol. 37, pp. 912–920.
11. Kreibig, U. and Vollmer, M., *Optical Properties of Metal Clusters*, New York: Springer, 1995.
12. Khlebtsov, N.G. and Dykman, L.A., *J. Quant. Spectr. Radiat. Transfer*., 2010, vol. 111, pp. 1–35.
13. Khlebtsov, N.G., Melnikov, A.G., Bogatyrev, V.A., and Dykman, L.A., *Photopolarimetry in Remote Sensing*, Videen, G., Yatskiv, Ya.S., and Mishchenko, M.I., Eds., NATO Science Series, II. Mathematics, Physics, and Chemistry, vol. 161, Dordrecht: Kluwer, 2004, pp. 265–308.
14. Khlebtsov, B.N., Zharov, V.P., Melnikov, A.G., Tuchin, V.V., and Khlebtsov, N.G., *Nanotechnology*, 2006, vol. 17, pp. 5167–5179.
15. Stockman, M.I., *Opt. Express*, 2011, vol. 19, pp. 22029–22106.
16. Ko, H., Singamaneni, S., and Tsukruk, V.V., *Small*, 2008, vol. 4, pp. 1576–1599.
17. Álvarez-Puebla, R.A. and Liz-Marzán, L.M., *Chem. Soc. Rev*., 2011, vol. 41, pp. 43–51.
18. Dieringer, J.A., McFarland, A.D., Shah, N.C., Stuart, D.A., Whitney, A.V., Yonzon, Ch.R., Young, M.A., Zhang, X., and Van Duyne, R.P., *Faraday Discuss*., 2006, vol. 132, pp. 9–26.
19. Henzie, J., Lee, J., Lee, M.H., Hasan, W., and Odom, T.W., *Annu. Rev. Phys. Chem*., 2009, vol. 60, pp. 147–165.
20. Natan, M.J., *Faraday Discuss*., 2006, vol. 132, pp. 321–328.
21. Alekseeva, A.V., Bogatyrev, V.A., Khlebtsov, B.N., Mel'nikov, A.G., Dykman, L.A., and Khlebtsov, N.G., *Colloid J*., 2006, vol. 68, pp. 661–678.
22. Zhao, Y.-P., Chaney, S.B., Shanmukh, S., and Dluhy, R.A., *J. Phys. Chem. B*., 2006, vol. 110, pp. 3153–3157.
23. Nikoobakht, B. and El–Sayed, M.A., *Chem. Mater*., 2003, vol. 15, pp. 1957–1962.
24. Dykman, L. and Khlebtsov, N., *Chem. Soc. Rev*., 2012, vol. 41, pp. 2256–2282.
25. Dreaden, E.C., Alkilany, A.M., Huang, X., Murphy, C.J., and El-Sayed, M.A., *Chem. Soc. Rev*., 2012, vol. 41, pp. 2740–2779.
26. Khlebtsov, B.N., Khanadeev, V.A., Panfilova, E.V., Minaeva, S.A., Tsvetkov, M.Y., Bagratashvili, V.N., and Khlebtsov, N.G., *Nanotechnol. in Russia,* 2012, vol. 7, pp. 359–369.
27. Khlebtsov, B.N., Panfilova, E.V., Terentyuk, G.S., Maksimova, I.L., Ivanov, A.V., and Khlebtsov, N.G., *Langmuir,* 2012, vol. 28, pp. 8994–9002.
28. Khlebtsov, B.N., Khanadeev, V.A., Panfilova, E.V., Pylaev, T.E., Bibikova, O.A., Staroverov, S.A., Bogatyrev, V.A., Dykman, L.A., and Khlebtsov, N.G., *Nanotechnol. in Russia*, 2013, vol. 8, pp. 209–219.

29. Khlebtsov, B., Khanadeev, V., and Khlebtsov, N., *Phys. Chem. C*, 2011, vol. 115, no. 14, pp. 6317–6323.
30. Ratto, F., Matteini, P., Rossi, F., and Pini, R., *J. Nanopart. Res*., 2010, vol. 12, pp. 2029–2036.
31. Schwartzberg, A.M., Grant, C.D., Wolcott, A., Talley, C.E., Huser, T.R., Bogomolni, R., and Zhang, J.Z., *J. Phys. Chem. B*, 2004, vol. 108, p. 19191–19197.
32. Hsiao, W.-H., Chen, H.-Y., Yang, Y.-C., Chen, Y., Lee, Ch.-Y., and Chiu, H.-T., *ACS Appl. Mater. Interfaces*, 2011, vol. 3, pp. 3280–3284.
33. Wang, Y., Guo, S., Chen, H., and Wang, E., *J. Colloid Interface Sci*., 2008, vol. 318, pp. 82–87.
34. Le Ru, E.C., Blackie, E., Meyer, M., and Etchegoin, P.G., *J. Phys. Chem. C*, 2007, vol. 111, pp. 13794–13803.
35. *http://www.renishawdiagnostics.com.*